REPORT DOCUMENTATION PAGE

Form Approved
OMB No. 0704-0188

The public reporting burden for this collection of information is estimated to average 1 hour per response, including the time for reviewing instructions, searching existing data sources, gathering and maintaining the data needed, and completing and reviewing the collection of information. Send comments regarding this burden estimate or any other aspect of this collection of information, including suggestions for reducing the burden, to Department of Defense, Washington Headquarters Services, Directorate for Information Operations and Reports (0704-0188), 1215 Jefferson Davis Highway, Suite 1204, Arlington, VA 22202-4302. Respondents should be aware that notwithstanding any other provision of law, no person shall be subject to any penalty for failing to comply with a collection of information if it does not display a currently valid OMB control number.

PLEASE DO NOT RETURN YOUR FORM TO THE ABOVE ADDRESS.

1. REPORT DATE *(DD-MM-YYYY)*	2. REPORT TYPE	3. DATES COVERED *(From - To)*
29-04-2011	Final	4/15/08-1/31/11

4. TITLE AND SUBTITLE
Modeling Density Variation in the Thermosphere

5a. CONTRACT NUMBER
FA9550-08-C-0046

5b. GRANT NUMBER

5c. PROGRAM ELEMENT NUMBER

6. AUTHOR(S)
Arthur Richmond

5d. PROJECT NUMBER

5e. TASK NUMBER

5f. WORK UNIT NUMBER

7. PERFORMING ORGANIZATION NAME(S) AND ADDRESS(ES)
University Corporation for Atmospheric Research
P.O. Box 3000
Boulder, Colorado 80307

8. PERFORMING ORGANIZATION REPORT NUMBER
2007-406 Final Technical ReportUU

9. SPONSORING/MONITORING AGENCY NAME(S) AND ADDRESS(ES)
USAF, AFRL
AF Office of Scientific Research
875 N. Randolph Street, Rm 3112
Arlington, VA 22203
Sandra Hudson

10. SPONSOR/MONITOR'S ACRONYM(S)

11. SPONSOR/MONITOR'S REPORT NUMBER(S)

12. DISTRIBUTION/AVAILABILITY STATEMENT
Publicly Available

13. SUPPLEMENTARY NOTES

14. ABSTRACT

The project objective was to significantly advance the quantitative understanding of solar and magnetospheric energy inputs to the upper atmosphere and the resultant responses of thermospheric density and wind and of ionospheric electron density. Specifically, our goals were to:

• Quantify the distribution of magnetospheric energy inputs to the thermosphere/ ionosphere system, and understand how energy is partitioned in terms of generating density and wind perturbations on local and global scales;

• Reveal and understand new aspects of the thermosphere response to solar extreme ultraviolet (EUV) variability, and how this response interacts with that to magnetospheric inputs;

• Develop improved parameters for first-principles models of the thermosphere/ionosphere system, in order to optimize their ability to simulate the system's response to variable energy inputs.

15. SUBJECT TERMS

16. SECURITY CLASSIFICATION OF:			17. LIMITATION OF ABSTRACT	18. NUMBER OF PAGES	19a. NAME OF RESPONSIBLE PERSON
a. REPORT	b. ABSTRACT	c. THIS PAGE			Ann Gumbiner
U	U	U	UU	14	19b. TELEPHONE NUMBER *(Include area code)* 303-497-2140

DEFENSE TECHNICAL INFORMATION CENTER

Information for the Defense Community

DTIC® has determined on 24 JUN 2011 that this Technical Document has the Distribution Statement checked below. The current distribution for this document can be found in the DTIC® Technical Report Database.

☒ **DISTRIBUTION STATEMENT A.** Approved for public release; distribution is unlimited.

☐ **© COPYRIGHTED**; U.S. Government or Federal Rights License. All other rights and uses except those permitted by copyright law are reserved by the copyright owner.

☐ **DISTRIBUTION STATEMENT B.** Distribution authorized to U.S. Government agencies only (fill in reason) (date of determination). Other requests for this document shall be referred to (insert controlling DoD office)

☐ **DISTRIBUTION STATEMENT C.** Distribution authorized to U.S. Government Agencies and their contractors (fill in reason) (date of determination). Other requests for this document shall be referred to (insert controlling DoD office)

☐ **DISTRIBUTION STATEMENT D.** Distribution authorized to the Department of Defense and U.S. DoD contractors only (fill in reason) (date of determination). Other requests shall be referred to (insert controlling DoD office).

☐ **DISTRIBUTION STATEMENT E.** Distribution authorized to DoD Components only (fill in reason) (date of determination). Other requests shall be referred to (insert controlling DoD office).

☐ **DISTRIBUTION STATEMENT F.** Further dissemination only as directed by (inserting controlling DoD office) (date of determination) or higher DoD authority.

Distribution Statement F is also used when a document does not contain a distribution statement and no distribution statement can be determined.

☐ **DISTRIBUTION STATEMENT X.** Distribution authorized to U.S. Government Agencies and private individuals or enterprises eligible to obtain export-controlled technical data in accordance with DoDD 5230.25; (date of determination). DoD Controlling Office is (insert controlling DoD office).

Modeling Density Variation in the Thermosphere

Final Report
Period of performance: 2008 April 15 - 2011 January 31

Arthur D. Richmond, Principal Investigator
High Altitude Observatory, National Center for Atmospheric Research
P.O. Box 3000, Boulder, CO 80307-3000

AFOSR Contract Number: FA9550-08-C-0046

20110624136

Project Objectives

The project objective was to significantly advance the quantitative understanding of solar and magnetospheric energy inputs to the upper atmosphere and the resultant responses of thermospheric density and wind and of ionospheric electron density. Specifically, our goals were to:

• Quantify the distribution of magnetospheric energy inputs to the thermosphere/ ionosphere system, and understand how energy is partitioned in terms of generating density and wind perturbations on local and global scales;

• Reveal and understand new aspects of the thermosphere response to solar extreme ultraviolet (EUV) variability, and how this response interacts with that to magnetospheric inputs;

• Develop improved parameters for first-principles models of the thermosphere/ionosphere system, in order to optimize their ability to simulate the system's response to variable energy inputs.

Work Carried Out and Results Obtained

1. Seasonal variation of thermospheric density and composition.

Qian et al. [2008] investigated the causes of seasonal variations in thermospheric neutral density and composition, which exhibit maximum densities near the equinoxes, a primary minimum during northern hemisphere summer, and a secondary minimum during southern hemisphere summer. This pattern of variation is described by thermospheric empirical models. However, the mechanisms are not well understood. The annual insolation variation due to the Sun-Earth distance can cause an annual variation; large-scale inter-hemispheric circulation can cause a global semiannual variation; and geomagnetic activity can also have a small contribution to the semiannual amplitude. However, simulations by the NCAR Thermosphere-Ionosphere-Electrodynamics General Circulation Model (TIE-GCM) indicate that these seasonal effects do not fully account for the observed annual/semiannual amplitude, primarily due to the lack of a minimum during northern hemisphere summer. A candidate for causing this variation is change in composition, driven by eddy mixing in the mesopause region. Other observations and model studies suggest that eddy diffusion in the mesopause region has a strong seasonal variation, with eddy diffusion larger during solstices than equinoxes, and stronger turbulence in summer than in winter. Qian et al. determined a seasonal variation of eddy diffusion that is compatible with this description. Simulations showed that when this function is imposed at the lower boundary of the TIEGCM, neutral density variation consistent with satellite drag data, and O/N_2 consistent with measurements by TIMED/GUVI, are obtained. These model-data comparisons and analyses indicate that transmission of turbulent mixing from the lower atmosphere may contribute to seasonal variation in the thermosphere, particularly the asymmetry between solstices that cannot be explained by other mechanisms.

2. Empirical model of high-latitude electrodynamics.

We developed empirical models of high-latitude electric potential, magnetic stream function, electric-field variability, and downward Poynting flux, based on measurements from the Dynamics-Explorer-2 spacecraft. Each model is a function of magnetic latitude and magnetic local time, and is parameterized in terms of hemisphere, dipole tilt angle toward the Sun (season), and magnitude and orientation of the interplanetary magnetic field (IMF). The models of electric potential and magnetic stream function are similar to comparable models by Weimer [Weimer, D.R. (2005), Improved ionospheric electrodynamic models and application to calculating Joule heating rates, J. Geophys. Res., 110, A05306, doi:10.1029/2004JA010884], but the models of electric-field variability and Poynting flux contain important additional information related to the variable components of the electric and magnetic fields about their climatological values. In particular, the variable field components produce an important additional energy input in the day-side high-latitude region. The empirical models are designed for use in simulation models of upper-atmospheric dynamics, as representations of the magnetospheric forcing and electromagnetic energy input. They have been used by Deng et al. [2009] to drive the TIE-GCM (see task 3). The component models have been prepared as computer subroutines that will be made available to the community after completion of testing and documentation. Examples of the fields predicted by these models over the northern polar region are shown in Figures 1-12 at the end of this report.

3. Impact of electric-field variability on the thermosphere.

Deng et al. [2009] used the empirical models of electric potential, electric-field variability, and downward Poynting flux described in task 2 as magnetospheric driving inputs to the TIE-GCM, to test how well the total Joule heating produced by the combined mean and variable components of the electric field agree with the independent estimate of this heating given by the Poynting flux. Whereas the TIE-GCM values of Joule heating depend on the ionospheric conductivity, the Poynting flux does not, and so these are two independent measures of the energy input to the thermosphere. Although some differences in spatial patterns of the Joule heating and Poynting flux were noted, the hemispherically integrated values agreed quite well, demonstrating that inclusion of the electric-field variability significantly improves our ability to estimate magnetospheric energy inputs to the thermosphere.

4. Dependence of the high-latitude thermospheric densities on the interplanetary magnetic field.

Kwak et al. [2009] carried out a systematic analysis of the interplanetary magnetic field (IMF) B_y and B_z influences on observed thermospheric density. For this purpose, the high-latitude southern summer thermospheric total mass density near 400 km altitude, derived from the high-accuracy accelerometer on board the Challenging Minisatellite Payload (CHAMP) spacecraft, was statistically analyzed in magnetic coordinates. The difference density distributions, obtained by subtracting values for zero IMF from these

for nonzero IMF, vary strongly with respect to the direction of the IMF: Difference densities for negative B_y show significant enhancements in the early morning hours and hours around dawn, but show reduced values in the dusk sector. For positive B_y the difference densities are opposite in sign to those for negative B_y. Density differences for negative B_z show significant increases in the cusp region and premidnight sector, but a small decrease in the dawn sector. The difference densities at high latitudes tend to be weakest when B_z is positive. The authors suggested that the high-latitude thermospheric density variations for different IMF conditions, especially in the dawn and dusk sectors, can be strongly determined by thermospheric winds, which are associated with the ionospheric convection and vary strongly with respect to the IMF direction. They also suggested that density variations, especially in auroral and cusp regions, are also influenced by the local heating associated with ionospheric currents, which vary with IMF conditions.

5. Thermospheric density enhancements in the dayside cusp region during strong IMF B_Y conditions.

Crowley et al. [2010] provided the first detailed explanation of a high-latitude density enhancement in the cusp sector observed in tri-axial accelerometer data from the Challenging Minisatellite Payload (CHAMP) satellite, focusing on the August 24, 2005 interval. The Thermosphere Ionosphere Mesosphere Electrodynamics General Circulation Model (TIMEGCM) was driven by high-fidelity high-latitude inputs specified by the Assimilative Mapping of Ionospheric Electrodynamics (AMIE) algorithm, and reproduced the main features of the density enhancements. The TIMEGCM and AMIE provide a global framework for interpretation of the CHAMP densities. The simulations reveal that the observed density enhancement in the dayside cusp region resulted from unexpectedly large amounts of energy entering the ionosphere-thermosphere system at cusp latitudes during an interval of strong (+20 nT) B_Y.

6. A computationally compact representation of Magnetic-Apex and Quasi-Dipole coordinates with smooth base vectors.

Many structural and dynamical features of the ionized and neutral upper atmosphere are strongly organized by the geomagnetic field, and are most conveniently represented with respect to magnetic coordinates. Modified Apex coordinates are appropriate for calculations involving electric fields and magnetic-field-aligned currents; Quasi-Dipole coordinates are appropriate for calculations involving height-integrated currents. Emmert et al. [2010] developed a compact, smooth, and robust representation of the transformation from geodetic to Quasi-Dipole and Modified Apex coordinates. They made the computer code available to the community for evaluating the coordinates and base vectors, as auxiliary material to their publication.

7. Model simulation of thermospheric response to recurrent geomagnetic forcing.

Qian et al. [2010] assessed model capability in simulating thermospheric response to recurrent geomagnetic forcing driven by modulations in the solar wind speed and the interplanetary magnetic field. Neutral density and nitric oxide (NO) cooling rates were

simulated for the declining phase of solar cycle 23. The simulated results are compared to neutral density derived from satellite drag and to NO cooling measured by the Thermosphere Ionosphere Mesosphere Energetics and Dynamics (TIMED) sounding of the atmosphere using broadband emission radiometry (SABER) instrument. Model-data comparisons show good agreement between the model and the measurements for multiday oscillations, as well as good agreement for longer-term variations. The simulations demonstrate that the multiday oscillation of density is globally distributed in the upper thermosphere but restricted to high latitudes in the lower thermosphere. The density variation in the upper thermosphere exhibits less latitude dependence than the temperature variation because of the effects of composition changes. Model simulations also show that NO density and temperature play primary roles in the multiday oscillation of NO cooling rates.

8. On the ionospheric application of Poynting's Theorem.

It has been proposed that the geomagnetic-field-aligned component of the perturbation Poynting vector above the ionosphere, as obtained from the cross product of the electric and magnetic-perturbation fields observed on a spacecraft, may be used to estimate the field-line-integrated electromagnetic energy dissipation in the ionosphere below. Richmond [2010] clarified conditions under which this approximation may be either valid or invalid. It was shown that the downward field-aligned component of the perturbation Poynting vector can underestimate the electromagnetic-energy dissipation in regions of high ionospheric Pedersen conductance, and it can significantly overestimate the dissipation in regions of low conductance. Local values of upward perturbation Poynting vector do not necessarily correspond to net ionospheric generation of electromagnetic energy along that geomagnetic-field line. An Equipotential-Boundary Poynting-Flux (EBPF) theorem was presented for quasi-static electromagnetic fields as follows: when a volume of the ionosphere is bounded on the sides by an equipotential surface and on the bottom by the base of the conducting ionosphere, then the area integral of the downward normal component of the perturbation Poynting vector over the top of that volume equals the energy dissipation within the volume. This equality does not apply to volumes with arbitrary side boundaries. However, the EBPF Theorem can be applied separately to different components of the electric potential, such as the large- and small-scale components. Since contours of the small-scale component of potential tend to close over relatively localized regions, the associated small-scale structures of downward perturbation Poynting vector tend to be dissipated locally.

9. Electrodynamics of ionosphere-thermosphere coupling.

Richmond [2011] presented an overview of ionosphere-thermosphere electrodynamic coupling. Collisions between the charged and neutral constituents of the upper atmosphere couple their respective dynamics and energetics. Magnetic stresses readily transfer momentum and energy over long distances along geomagnetic-field lines, accompanied by electric fields and currents. Consequently, the E and F regions of the ionosphere are strongly coupled, and momentum is transferred between the lower and upper thermosphere through the currents and their associated ion drag. Electrical

conductivity mediates the degree of ion-neutral coupling. Conductivity is highly variable, and is itself affected by the electric field in various ways. Thermospheric winds drive the ionospheric wind dynamo. The winds are created by daily absorption of solar radiation in the thermosphere, by upward propagating solar and lunar tides, by ion-drag acceleration at high latitudes, and by Joule heating at high latitudes. Electric current flows globally in the ionosphere and along geomagnetic-field lines through the magnetosphere. Interactions between the ion and neutral motions produce feedbacks that affect the dynamics of both components. Simulation models of thermosphere-ionosphere-electrodynamic interactions provide powerful tools for investigating the nature of these interactions, and for testing how well the uncertain model inputs and the physics incorporated in the models are able to predict observed features of the ionosphere and thermosphere.

10. Thermospheric mass density: an overview of temporal and spatial variations.

Qian and Solomon [2011] summarized and discussed thermospheric density variations, their magnitudes, and their forcing mechanisms, using neutral density data sets and modeling results. The density data sets included observations by accelerometers on the Challenging Mini-satellite Payload (CHAMP) and measurements of orbit changes on other space objects due to drag at perigee, and global-mean density derived from thousands of orbiting objects. Modeling results are from the TIE-GCM and from the NRLMSISE-00 empirical model. Neutral density shows complicated temporal and spatial variations driven by external forcing of the thermosphere/ionosphere system, internal dynamics, and thermosphere and ionosphere coupling. Temporal variations include abrupt changes with a time scale of minutes to hours, diurnal variation, multi-day variation, solar-rotational variation, annual/semiannual variation, solar-cycle variation, and long-term trends with a time scale of decades. Spatial variations include latitudinal and longitudinal variations, as well as variation with altitude. Atmospheric drag on satellites varies strongly as a function of thermospheric mass density. Errors in estimating density cause orbit prediction error, and impact satellite operations, including accurate catalog maintenance, collision avoidance for manned and unmanned space flight, and re-entry prediction.

People Involved

Those receiving direct support from the funding were:
Art Richmond (PI)
Stan Solomon (Co-I)
Astrid Maute (Collaborator)
Liying Qian (Collaborator)
Delores Knipp (NCAR/HAO Senior Research Associate)
Ben Foster (NCAR/HAO Software Engineer)
Joe McInerney (NCAR/HAO Associate Scientist).

We collaborated with many scientists participating in the MURI project "Neutral Atmosphere Density Interdisciplinary Research" (NADIR), including:

Jeff Forbes (U. Colorado)
Tim Fuller-Rowell (U. Colorado)
Jeff Thayer (U. Colorado)
Tomoko Matsuo (U. Colorado)
Jiuhou Lei (U. Colorado)
Geoff Crowley (ASTRA).

Other scientists involved include:
Yue Deng (NCAR/HAO postdoc)
Doug Drob (Naval Research Laboratory)
John Emmert (Naval Research Laboratory)
Kelly Ann Drake (USAF Academy contractor)
Tim Kane (Pennsylvania State University)
Young-Sil Kwak (Korea Astronomy and Space Science Research Institute)
Hermann Lühr (Geoforschungszentrum Potsdam)
Marty Mlynczak (NASA Langley SFC)
Ray Roble (NCAR/HAO)
Eric Sutton (AFRL).

Publications

Crowley, G., D.J. Knipp, K.A. Drake, J. Lei, E. Sutton, and H. Lühr (2010), Thermospheric density enhancements in the dayside cusp region during strong B_Y conditions, Geophys. Res. Lett., 37, L07110, doi:10.1029/2009GL042143.

Deng, Y., A. Maute, A.D. Richmond, and R.G. Roble (2009), Impact of electric field variability on Joule heating and thermospheric temperature and density, Geophys. Res. Lett., 36, L08105, doi:10.1029/2008GL036916.

Emmert, J.T., A.D. Richmond, and D.P. Drob (2010), A computationally compact representation of Magnetic-Apex and Quasi-Dipole coordinates with smooth base vectors, J. Geophys. Res., 115, A08322, doi:10.1029/2010JA015326.

Kwak, Y.-S., A. Richmond, Y. Deng, J. Forbes, and K.-H. Kim (2009), Dependence of the high-latitude thermospheric densities on the interplanetary magnetic field, J. Geophys. Res., 114, A05304, doi:10.1029/2008JA013882.

Qian, L., and S.C. Solomon (2011), Thermospheric mass density: an overview of temporal and spatial variations, Space Sci. Rev., submitted.

Qian, L., S.C. Solomon, and T.J. Kane (2009), Seasonal variation of thermospheric density and composition, J. Geophys. Res., 114, A01312, doi:10.1029/2008JA013643.

Qian, L., S.C. Solomon, and M.G. Mlynczak (2010), Model simulation of thermospheric response to recurrent geomagnetic forcing, J. Geophys. Res., 115, A10301, doi:10.1029/2010JA015309.

Richmond, A.D. (2010), On the ionospheric application of Poynting's Theorem, J. Geophys. Res., 115, A10311, doi:10.1029/2010JA015768.

Richmond, A.D. (2011), Electrodynamics of ionosphere-thermosphere coupling, in Aeronomy of the Earth's Atmosphere and Ionosphere, edited by M.A. Abdu, D. Pancheva, and A. Bhattacharyya, Springer, Dordrecht, pp. 191-201.

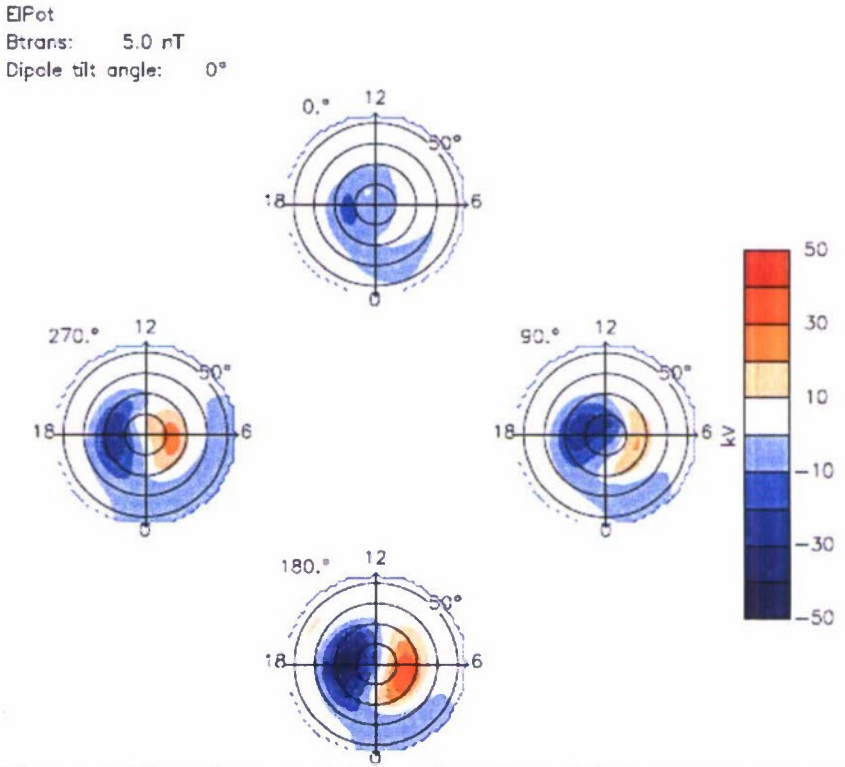

Figure 1. Electric potential as a function of IMF clock angle for a transverse IMF magnitude of 5 nT and for zero dipole tilt.

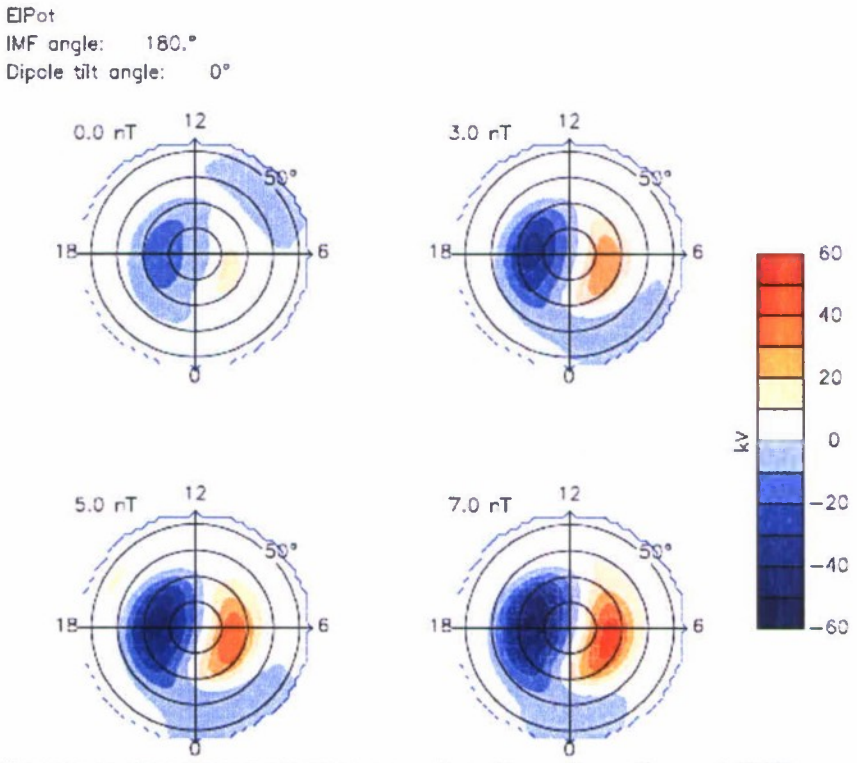

Figure 2. Electric potential as a function of southward IMF magnitude for zero dipole tilt.

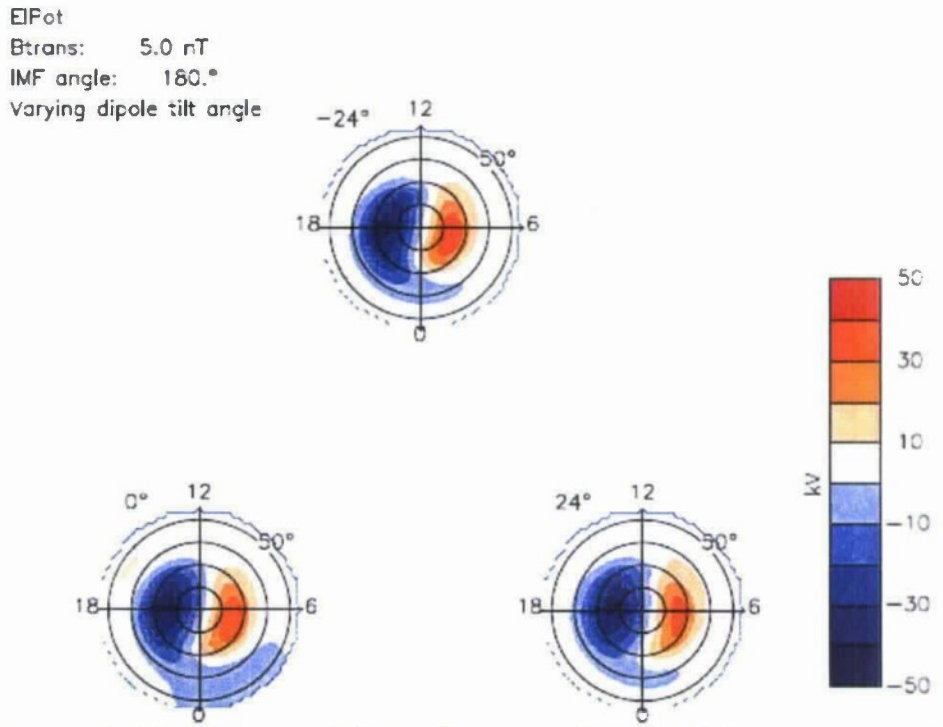

Figure 3. Electric potential as a function of dipole tilt for a southward IMF of 5 nT.

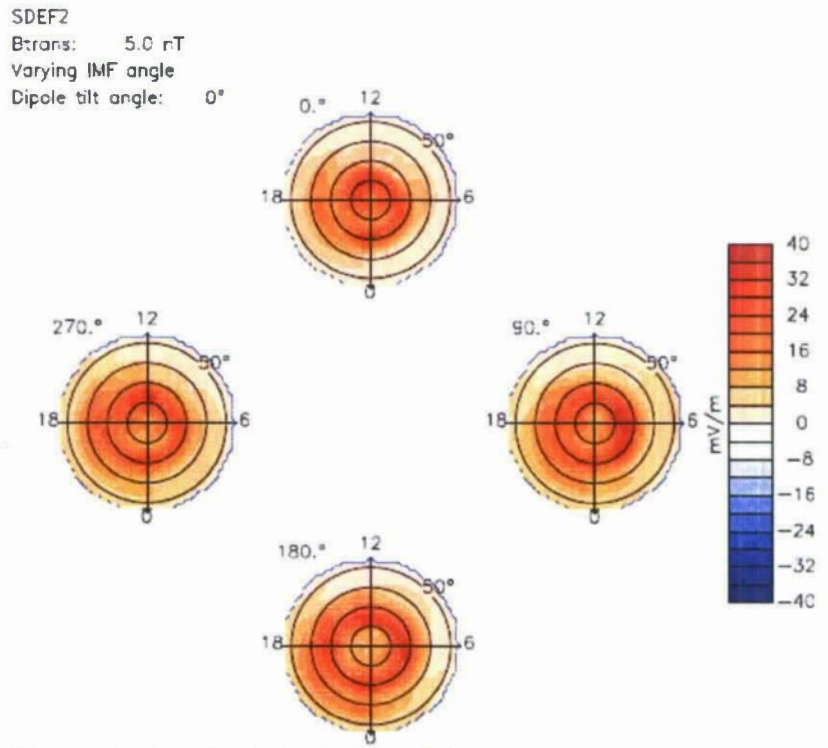

Figure 4. Standard deviation of the northward electric field as a function of IMF clock angle for a transverse IMF magnitude of 5 nT and for zero dipole tilt.

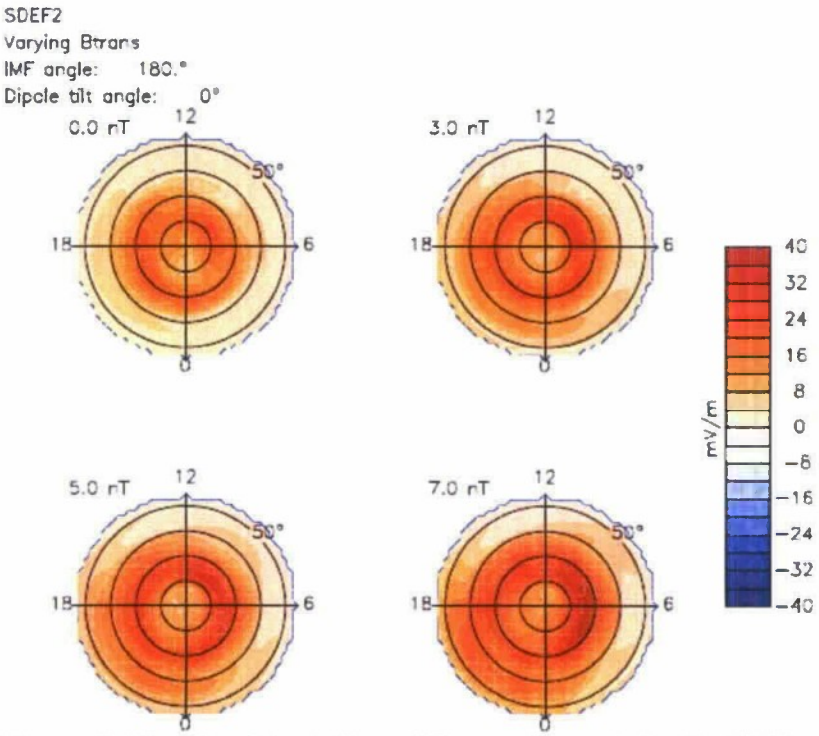

Figure 5. Standard deviation of the northward electric field as a function of southward IMF magnitude for zero dipole tilt.

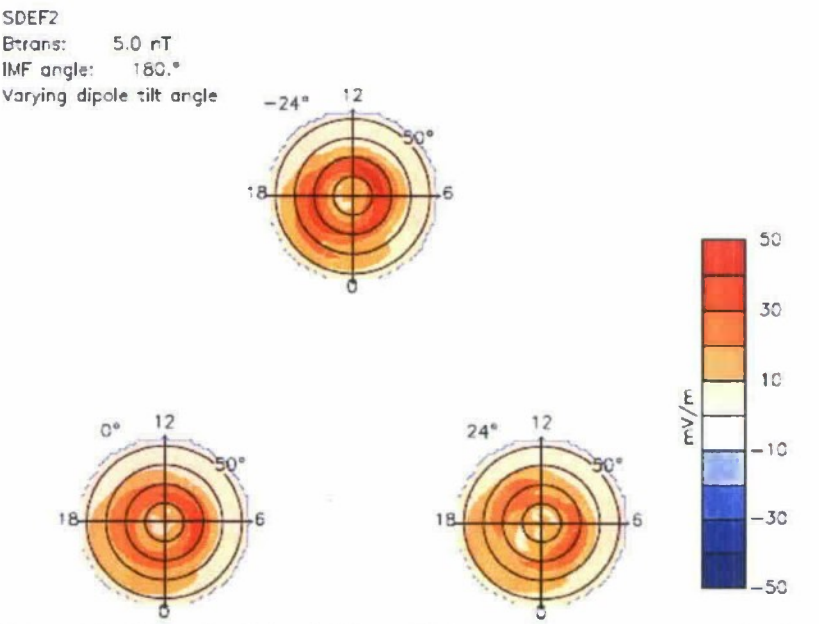

Figure 6. Standard deviation of the northward electric field as a function of dipole tilt for a southward IMF of 5 nT.

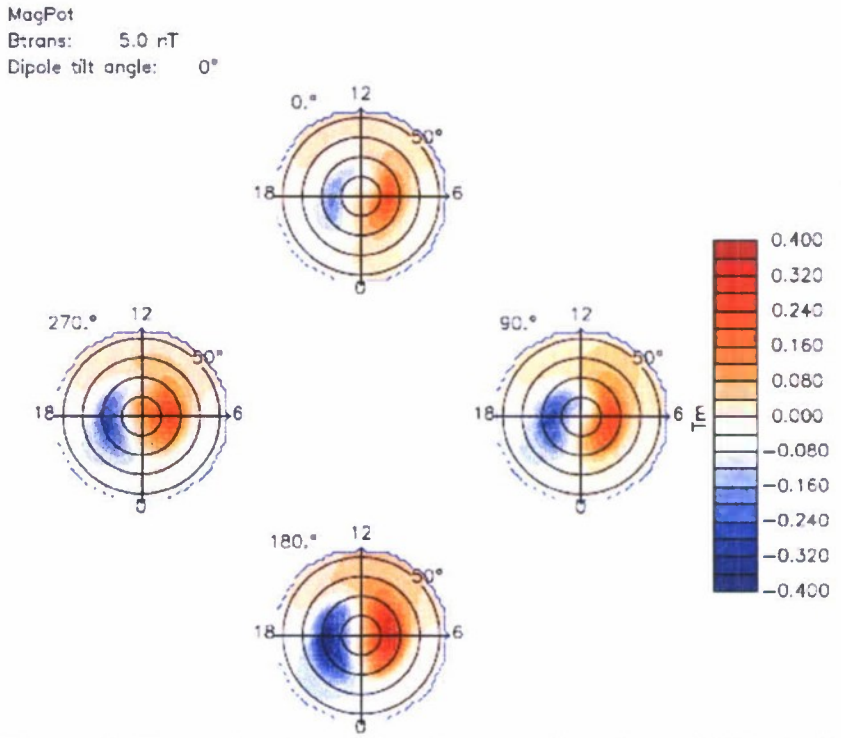

Figure 7. Magnetic stream function as a function of IMF clock angle for a transverse IMF magnitude of 5 nT and for zero dipole tilt.

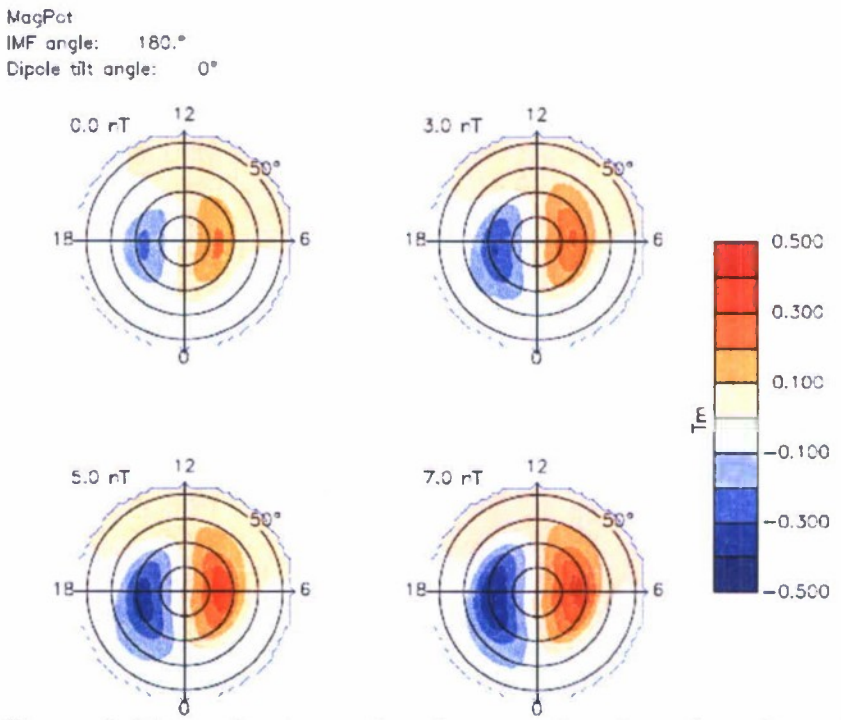

Figure 8. Magnetic stream function as a function of southward IMF magnitude for zero dipole tilt.

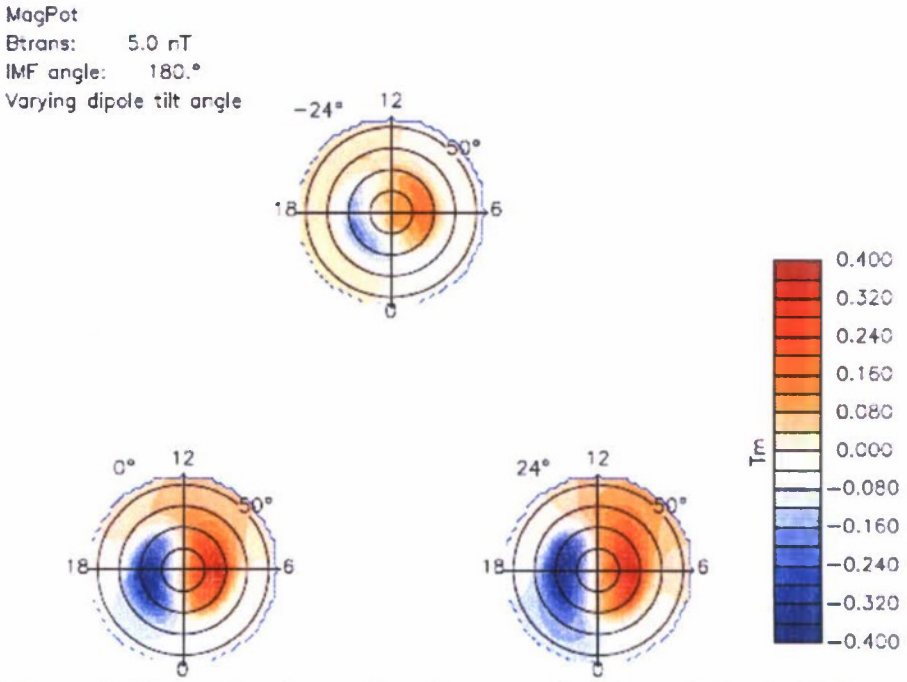

Figure 9. Magnetic stream function as a function of dipole tilt for a southward IMF of 5 nT.

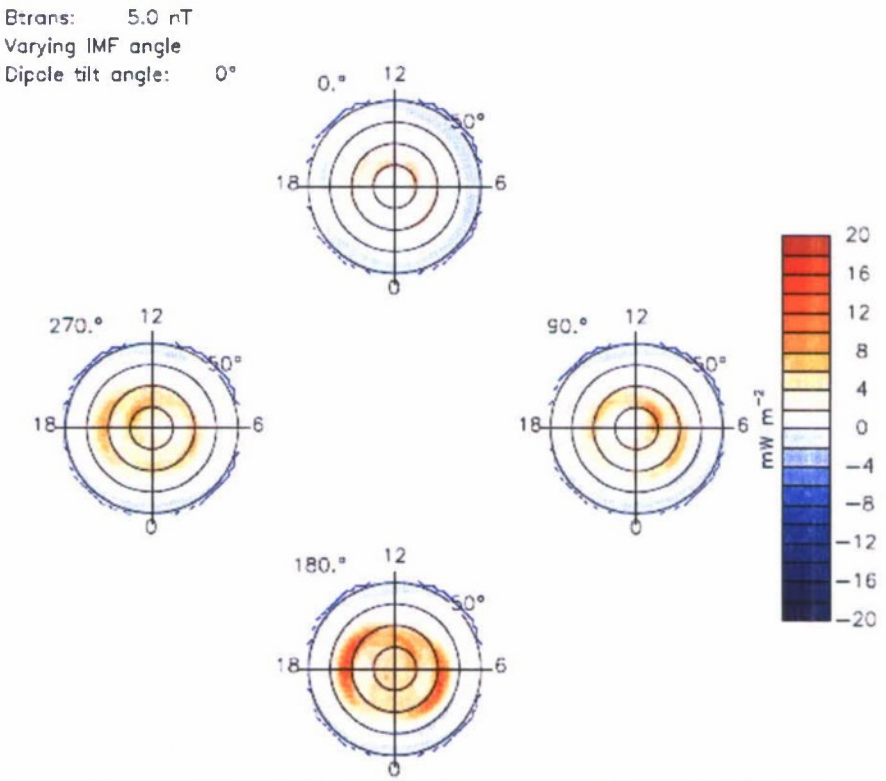

Figure 10. Downward Poynting flux as a function of IMF clock angle for a transverse IMF magnitude of 5 nT and for zero dipole tilt.

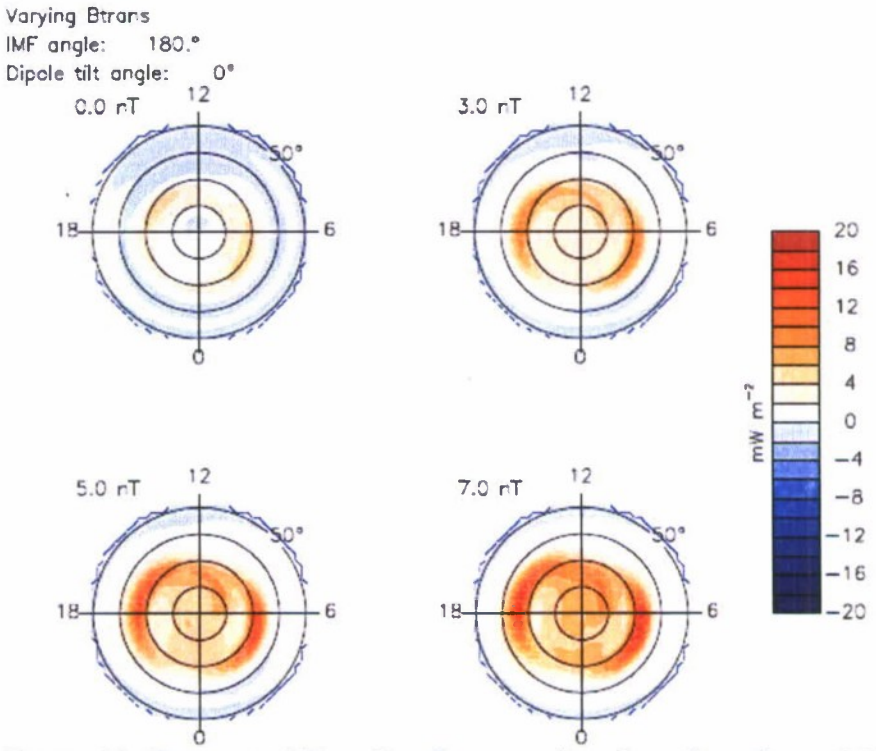

Figure 11. Downward Poynting flux as a function of southward IMF magnitude for zero dipole tilt.

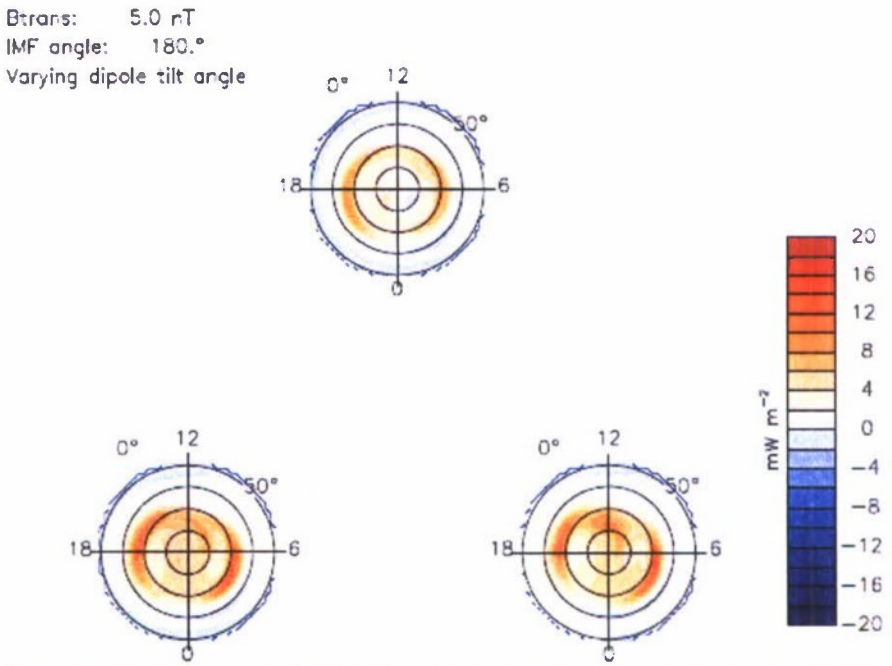

Figure 12. Downward Poynting flux as a function of dipole tilt for a southward IMF of 5 nT. (The top plot is for -24^0 tilt, the lower-left plot is for 0^0, and the bottom-right plot is for +24^0 tilt.)